First-principles calculations of surfactant-assisted growth of polar CaO(111) oxide film: The case of water-based surfactant

Xin Tan and Peter Zapol*
Materials Science Division, Argonne National Laboratory, Argonne, Illinois 60439, USA
(Received 19 April 2012; published 16 July 2012)

Surfactant-assisted growth of polar CaO(111) oxide film in the presence of water-based surfactant is studied by first-principles calculations both from thermodynamic and kinetic points of view. We show that the water molecules not only supply a surfactant by depositing hydrogen on the surface throughout the growth process, but also supply oxygen atoms as an elemental constituent in the film growth with rather small energy barriers, i.e. water oxygen atoms are easily inserted in the top surface layer of the growth film during the wet oxidation process. Adding the water surfactants to conventional synthesis techniques leads to the continuous presence of hydrogen atoms in the surface region during the growth process, which efficiently quenches polarity and dynamically stabilizes the growth of the polar surface, and thus facilitates the growth of defect-free CaO(111) films with arbitrary thickness.

DOI: 10.1103/PhysRevB.86.045422 PACS number(s): 68.43.Bc, 68.47.Gh, 82.65.+r, 68.35.Ct

I. INTRODUCTION

Polar surfaces of metal oxides and compound semiconductors are of prominent interest in mineralogy, geochemistry, catalysis, electrochemistry, electronics, and magnetic recording.[1,2] One of the simplest polar structures is a polar (111) metal monoxide film with rocksalt structure, such as MgO, NiO, CaO, or BaO, consisting of oppositely charged metal and oxygen atom layers alternatively stacked along the [111] direction. Such a structural arrangement of uncompensated stoichiometric film leads to a divergence of the dipole moment, electrostatic potential, and surface energy with increasing film thickness, making the rocksalt (111) surface highly unstable.[3] An electrostatic instability that results from the presence of this macroscopic dipole can be cancelled either by a deep modification of the surface electronic structure—surface metallization—or by strong changes in the surface stoichiometry—surface faceting, surface reconstructions, or changes to surface composition.[4–6] Although many attempts have been made to grow rocksalt (111) surfaces using layer-by-layer molecular beam epitaxy (MBE) and atomic layer deposition (ALD),[7–9] the growth of an atomically flat polar oxide film with an arbitrary thickness still remains challenging because of surface roughening during the growth process, such as faceting into neutral {100} surface planes, which appears to be one mechanism for overcoming polarity.[4,5] This seemingly unavoidable behavior leads to a grainy morphology and diminished functionality.

Recently, Lazarov *et al.*[10] have employed first-principles calculations predicting the surfactant-assisted growth of single-crystal polar MgO(111) film of arbitrary thickness using hydrogen as a surfactant, which has been confirmed experimentally by single-crystal growth of MgO(111) on SiC(0001). The surfactant hydrogen changes its position and remains on the surface during the growth process, providing a dynamic solution for the polarity constraints throughout the growth of MgO(111), by effectively healing (quenching) the surface dipole moment and thus lowering the surface energy. At the same time, in the presence of a water-based surfactant, Paisley *et al.*[11] have demonstrated the surfactant-assisted growth of atomically flat polar CaO(111) oxide film with arbitrary thickness by MBE growth of CaO(111) on GaN(0001). In addition, they have used *ab initio* thermodynamic calculations to predict that, in the presence of the water surfactant, flat CaO(111) surfaces are stabilized by hydroxylation during surfactant-assisted growth at temperatures below 253 °C. However, the water-based surfactant-assisted growth mechanism remains unknown. In particular, how does the water molecule act as a surfactant, and how is a water oxygen atom inserted into the top surface layer of the growth film during wet oxidation process? These are questions that can be addressed through first-principles calculations from a kinetic point of view.[12]

In this paper, we present a first-principles investigation of the surfactant-assisted growth of polar CaO(111) film in the presence of a water-based surfactant, both from thermodynamic and kinetic points of view. By means of simulating alternate Ca deposition and wet oxidation of a CaO(111) surface, we can calculate the binding energies, stable configurations, energy barriers, and reaction pathways related to the growth process. The results show that the water molecules not only play the role of surfactant, remaining on the surface throughout the growth process, but also supply oxygen atoms as an elemental constituent in film growth with rather small energy barriers, i.e. water oxygen atoms are easily inserted in the top surface layer of the growing film during the wet oxidation process. Introducing water surfactants to conventional synthesis techniques induces the continuous presence of hydrogen atoms on the surface during the growth process. The surface hydrogen atoms efficiently heal polarity and dynamically stabilize the growth of polar surface and thus facilitate the growth of smooth CaO(111) films with arbitrary thicknesses.

II. METHODS

In order to simulate the surfactant-assisted growth of polar CaO(111) oxide films in the presence of a water-based surfactant, we performed a series of density functional theory (DFT) calculations starting from the deposition of its elemental constituents on OH-terminated CaO(111), as shown in Fig. 1. The hydroxylated CaO(111) surface was calculated to have the

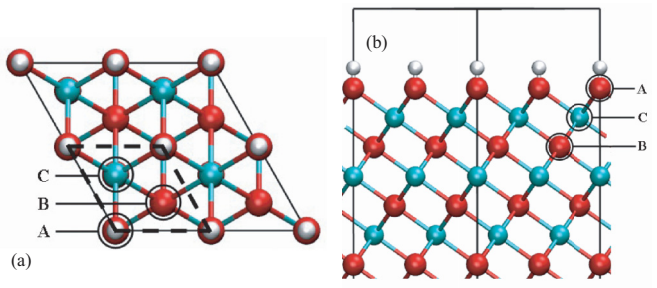

FIG. 1. (Color online) (a) Top view and (b) side view of the OH-terminated CaO(111) surface. In (a) and (b), three possible adsorption sites (A, B, and C) are indicated. The (1 × 1) surface unit cell is shown by the black dashed line in (a). Big blue (bright) spheres: Ca, big red (dark) spheres: O, small gray (bright) spheres: H.

lowest surface free energy up to 253 °C and was experimentally observed during the surfactant-assisted growth.[11] Two crucial steps were investigated to understand the growth process: (i) the arrival of the first Ca atomic layer and then (ii) the subsequent water oxygen atom insertion into the CaO(111) top surface layer.

Our DFT calculations were performed with the VASP program[13] using a plane-wave basis set and a projector augmented wave method (PAW) for the treatment of core electrons.[14] The Perdew–Burke–Ernzerhof (PBE)[15] form of the generalized gradient approximation (GGA) exchange-correlation functional was used in all calculations. For the expansion of the plane-wave basis set, a converged cutoff was set to 500 eV. The calculated CaO bulk lattice constant is 4.830 Å, which is in good agreement with the experimental value of 4.803 Å.[16] The OH-terminated CaO(111) surfaces were modeled with periodic supercells, containing a vacuum region 22-Å thick and a slab consisting of 13 atomic layers constructed to have inversion symmetry, i.e the top and bottom surface have the same termination and are passivated with hydrogen atoms, which avoids artificial dipole-dipole interactions between the periodically repeated supercells. The minimum lateral periodicity we used was the (1 × 1) surface unit cell [Fig. 1(a)], and for specific cases, we extended the simulations to (2 × 2) surface unit cells. The Brillouin zone integration was performed on a (12 × 12 × 1) Monkhorst–Pack k-point mesh[17] for the (1 × 1) surface unit cell. Only one side of this slab was used to adsorb Ca atoms and to react with water molecules in our calculations. In geometry optimizations, all the atomic coordinates were fully relaxed up to the residual atomic forces smaller than 0.02 eV/Å. Binding energies and reaction energies were obtained by taking the difference between the total energy of the initial structure and that of the final structure.

The energy barriers, transition states, and reaction pathways related to water molecule dissociation and water oxygen atom insertion into the CaO(111) top surface layer were obtained using the method known as climbing image-nudged elastic band (CI-NEB).[18] The method searches for the so-called minimum energy pathway (MEP) of a reaction by optimizing a constructed string of intermediate configurations (images) to pass through the transition state, which only requires *a priori* structural information of the initial and final states. It is thus a suitable technique for efficiently exploring a large region of configuration space to find an MEP. In order to accurately describe the reaction pathways, we used seven intermediate images, allowing all atoms to move within the CI-NEB optimization process.

III. RESULTS AND DISCUSSION

A. The arrival of the first Ca atomic layer

The natural choice for simulating CaO(111) growth at the OH-terminated CaO(111) surface described above is to start with the adsorption of Ca atoms. Three possible adsorption sites, A, B, and C, on the OH-terminated CaO(111) surfaces are shown in Fig. 1. The DFT optimized structures and the corresponding binding energies for Ca atoms adsorbed at these sites are shown in Fig. 2. Our calculations show that the most stable adsorption site is the B site, as shown in Fig. 2(b). The binding energy of the Ca atom at the B site is rather large 3.44 eV; the corresponding energies for the A and C sites are 0.91 and 3.12 eV, respectively. The optimized structures of Figs. 2(b) and 2(c) suggest a growth scenario in which an exchange mechanism is at work: when Ca atoms arrive at a B or C site, the deposited Ca atoms penetrate into the top surface layer, and the two surface hydrogen atoms break the O-H bond and spontaneously move upwards to 1.12 and 1.11 Å above the newly formed Ca layer, but still at A sites. The OH-terminated CaO(111) surface therefore changes to an H-Ca-terminated surface. This is very similar to the case of Mg deposition on an OH-terminated MgO(111) surface.[10]

In order to investigate the adsorption configurations of Ca atoms on OH-terminated CaO(111) surfaces at different dosages, we use a larger in-plane cell size, i.e. (2 × 2) surface supercell, to optimize structures with a partial Ca coverage on the most stable adsorption site, i.e. the B site, of the OH-terminated CaO(111) surface. As illustrated in Figs. 3(a) and 3(b) for the low Ca coverages (1/4 and 1/2 ML, respectively), the Ca atoms adsorb above the hydrogen layer and slightly push away the nearest hydrogen

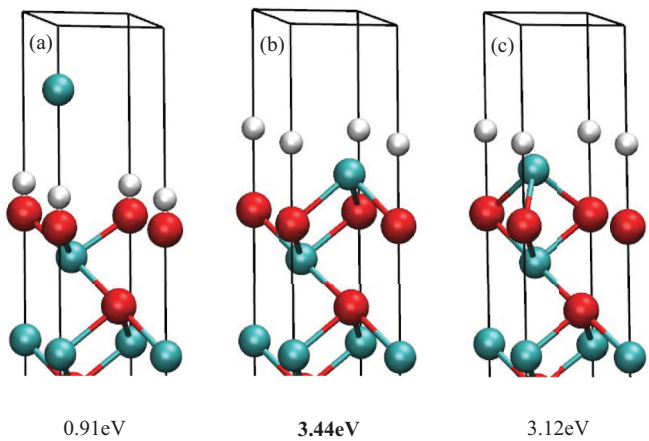

FIG. 2. (Color online) Perspective view of the Ca atomic adsorption geometry on (a) A, (b) B, and (c) C sites at the OH-terminated CaO(111) surface. The corresponding binding energies of the Ca atom are also shown, and the binding energy of the most stable configuration is in bold.

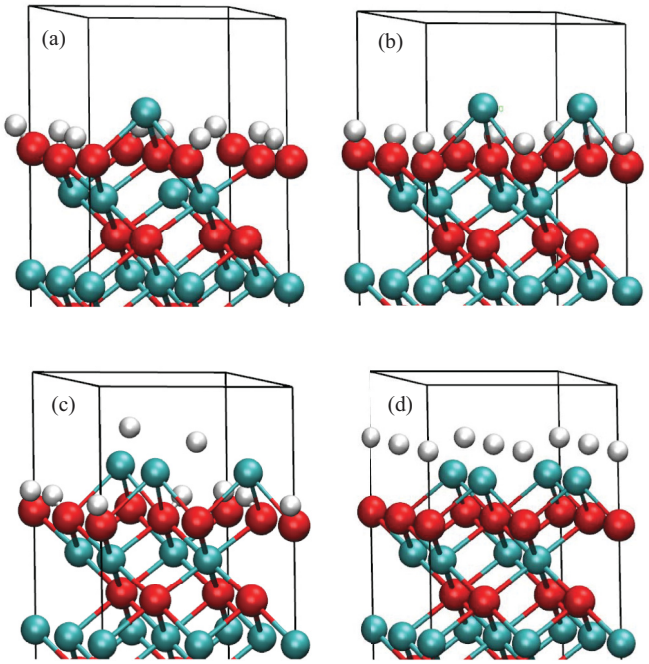

FIG. 3. (Color online) Perspective view of optimized surface geometry after deposition of (a) 1/4-, (b) 1/2-, (c) 3/4-, and (d) 1-ML Ca atoms at the OH-terminated CaO(111) surface.

atoms. As the Ca coverage increases to 3/4 ML [see Fig. 3(c)], the hydrogen atom that has the three nearest B sites occupied by Ca atoms breaks the O-H bond and spontaneously moves upwards to 1.15 Å above the newly formed Ca layer, leaving the other three hydrogen atoms below the newly formed Ca layer. With Ca coverage increase to 1 ML [Fig. 3(d)], all of the surface hydrogen atoms spontaneously exchange positions with deposited Ca atoms and move above the newly formed Ca layer. These growth features are different from the case when Mg atoms are deposited on OH-terminated MgO(111) surface. In the latter case, the hydrogen atoms move upwards above the newly formed Mg layer starting at 1/2 ML Mg deposition.[10]

To better understand the H-Ca-terminated CaO(111) surface described above, we identify the most stable surface configuration after the arrival of the first Ca atomic layer through a comparative study of the binding energy of surface hydrogen atom at different sites. Figure 4 shows the DFT optimized configurations and the binding energies of a surface hydrogen atom at different sites. The hydrogen atom at the C site is the most stable shown in Fig. 4(c), and its binding energy is rather large 3.56 eV/unit cell, which is 0.38 and 2.22 eV/unit cell larger than that at the A and B sites, respectively. For the case of the surface hydrogen atom adsorbed at the C site, the interlayer spacing between the surface hydrogen layer and Ca layer is small 1.00 Å, which is 0.13 and 0.98 Å smaller than that at the A and B sites, respectively. After the arrival of the first Ca atomic layer, it is not energetically favorable for surface hydrogen atoms to remain at the A site, preferring the C site. Thus, the newly formed H-Ca-terminated CaO(111) surface configuration is H(C)/Ca(B)/O(A) . . .

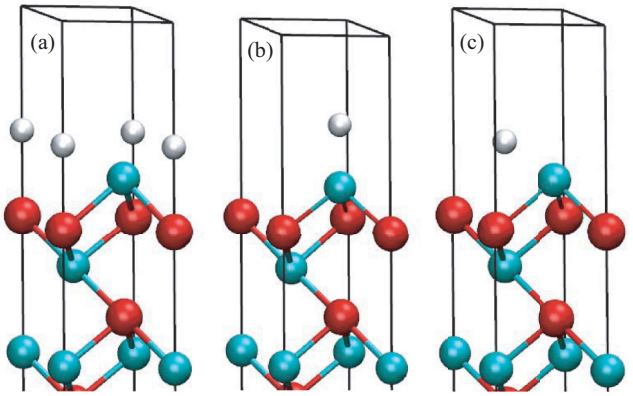

FIG. 4. (Color online) Perspective view of the surface geometries of the H-Ca-terminated CaO(111) surface with hydrogen atom at (a) A, (b) B, and (c) C sites. The corresponding binding energies of surface hydrogen atom are also listed in this picture, and the binding energy of the most stable configuration is in bold.

B. Water oxygen atom insertion in the H-Ca-terminated CaO(111) top surface layer at wet oxidation

As the water vapor is the sole oxidant of the H-Ca-terminated CaO(111) surface, we examined the dissociation of the water molecule and whether the oxygen atom is inserted into the top surface layer of the growing film. First, we address the initial and final configurations of the water molecule on the H-Ca-terminated CaO(111) surface. We looked for the metastable binding locations for a water molecule by locating the most likely adsorption sites on the surface and then relaxing the structure to each nearest local minimum of the potential energy surface (PES). As we can see from Figs. 5(a)–5(c), the water molecule is physisorbed at three possible sites on the H-Ca-terminated surface, and the binding energies of the water molecule at the A, B, and C sites are 0.10, 0.24, and 0.12 eV, respectively. The structures of water molecule adsorption at the A or B site have geometries with the water oxygen atom directly above the A or B site and the water hydrogen atoms in the same plane that are directed towards two of the three nearest C sites. For water molecule adsorption at the C site, the water oxygen atom moves above the center of the ABC triangle. One water hydrogen atom is directed towards the C site, and the other water hydrogen atom is located above the water oxygen atom. As the difference of binding energies between the three physisorbed situations of the water molecule discussed above is small ($0.10 \sim 0.24$ eV), it does not allow us to distinguish them by stability. In this case, we consider the three physisorbed geometries as the initial configurations of water molecule physisorption on the H-Ca-terminated CaO(111) surface.

The most interesting result is the first-principles relaxed structure for the chemisorbed configuration: when the water molecule dissociates, the water OH group occupies the C site, a site where initially a surface hydrogen sits, and an H_2 molecule is released [Fig. 5(d)]. The OH group is chemisorbed at the C site in the final configuration, and the reaction energy for water is rather large 1.78 eV, which is $1.54 \sim 1.68$ eV more favorable than the physisorbed configurations. This suggests that the dissociated configuration is thermodynamically favorable

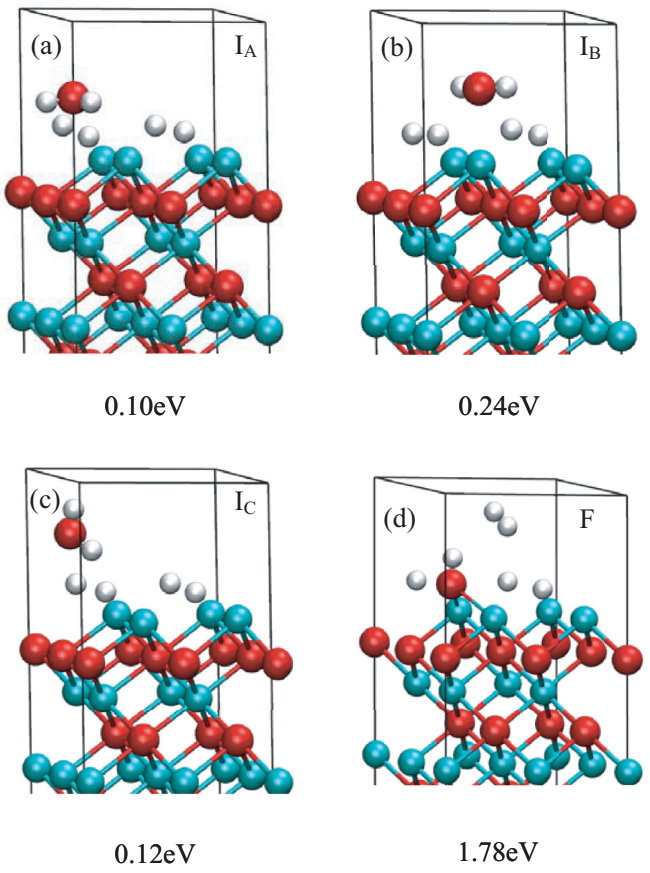

FIG. 5. (Color online) Perspective view of the water molecule physisorbed geometries (I_A, I_B, I_C) on the H-Ca-terminated CaO(111) surface with the water molecule at (a) A, (b) B, and (c) C sites. (d) Perspective view of the water molecule chemisorbed geometry (F) on the H-Ca-terminated CaO(111) surface. The corresponding binding energies of the water molecule on the surface are also shown.

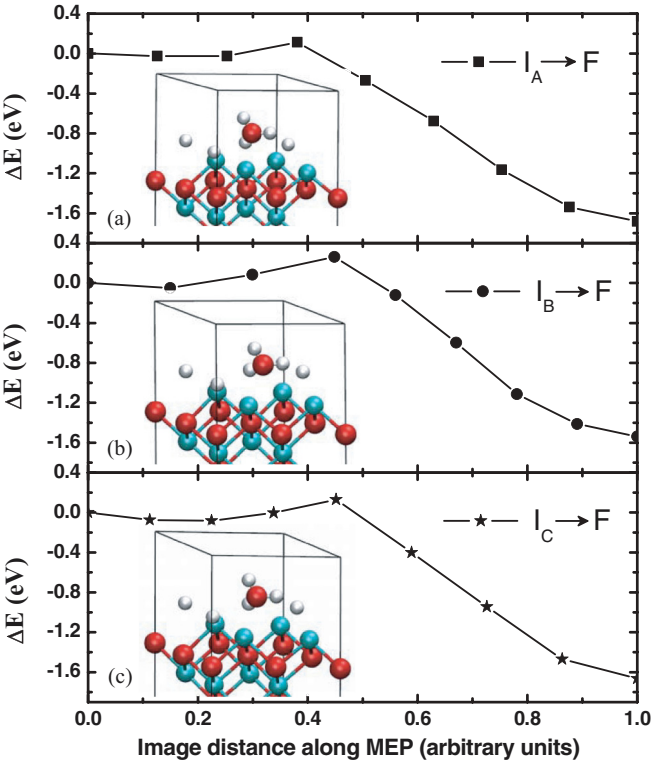

FIG. 6. (Color online) Different MEP for the water molecule at (a) A, (b) B, and (c) C sites dissociation and water oxygen atom insertion in the H-Ca-terminated surface region during wet oxidation. Insets show the transition states of each reaction pathway.

compared to the physisorbed configurations in the wet oxidation process. In this way, the water oxygen atom is inserted into the top surface layer, and the hydrogen atoms continuously reside on the surface throughout the wet oxidation process. In order to investigate how many water oxygen atoms can be inserted into the top surface layer, we calculated the reaction energy of the insertion of four water molecules in the top surface layer. This is a highly exothermic reaction, with 1.62 eV evolved per water molecule. This suggests that more water molecules can dissociate, and OH groups occupy all the C sites on the H-Ca-terminated CaO(111) surface. Therefore, after the deposition of the Ca layer and the wet oxidation process, the surface atomic configuration is identical to the one before the onset of the film growth, i.e. the OH-terminated CaO(111) shown in Fig. 1.

To gain insight into the kinetics of the wet oxidation process, we calculated the energy barriers and the reaction pathways related to water molecule dissociation and water oxygen atom insertion into an H-Ca-terminated surface region at wet oxidation, using the initial and final configurations described above. By means of the CI-NEB method, we were able to find the MEP connecting the initial and final state of each reaction pathway. The calculation results show that the reaction scenarios and the transition states for the three possible reaction pathways are very similar, as shown in Fig. 6: The water molecule dissociates into an OH group and a hydrogen atom. In this process, the OH group moves to the C site, a site where surface hydrogen sits initially. At the same time, the water hydrogen atom combines with this surface hydrogen atom resulting in a release of an H_2 molecule. The energy barriers for three reaction pathways are rather small, 0.14, 0.31, and 0.21 eV, respectively, suggesting that a water molecule can easily dissociate, and a water oxygen atom can be easily inserted into an H-Ca-terminated surface during the wet oxidation process at the experimental conditions, from 150 to 450 °C.[11]

Now, the presented calculations clearly show the growth scenario of surfactant-assisted growth in the presence of a water-based surfactant: on an OH-terminated CaO(111) surface, the surface hydrogen atoms spontaneously exchange position with the first deposited Ca atoms and locate above the newly formed Ca layer starting at the Ca coverage of 3/4 ML. Subsequently, the H-Ca-terminated CaO(111) surface undergoes oxidation in the presence of the water surfactant with energy barriers of 0.14 ∼ 0.31 eV. The water surfactant dissociates into an OH group and a hydrogen atom. The OH group moves to the C site, resulting in water oxygen atom insertion into the surface of the film. At the same time, a water hydrogen atom combines with a surface hydrogen atom originally at the C site resulting in a release of an H_2 molecule. Though the energy barrier for dissociation of a

water surfactant at wet oxidation is rather small, we expect a failure to achieve a defect-free polar CaO(111) oxide film when the sample temperature is too low or the Ca deposition rate is too high. For common experimental conditions (above room temperatures), we expect the growth temperature is high enough to achieve a defect-free polar CaO(111) oxide film. On the other hand, as the water vapor is the sole oxidant of the H-Ca-terminated CaO(111) surface, a very low water partial pressure cannot supply enough oxygen atoms during the growth process, leading to a transition to Ca metal deposition. In addition, as surface faceting and a grainy morphology have been observed in the preparation of other thin polar films, we expect that the results in this paper could be useful to investigate the growth of other polar surfaces, such as for metal oxides with perovskite structures.

IV. SUMMARY AND CONCLUSION

In conclusion, we have used first-principles calculations to systematically investigate the surfactant-assisted growth of defect-free polar CaO(111) oxide film in the presence of water by means of alternate Ca deposition and wet oxidation of an H-Ca-terminated CaO(111) surface. Our calculations demonstrate that the water molecules not only play the role of a surfactant, by depositing hydrogen on the surface throughout the growth process, but also supply water oxygen atoms as an elemental constituent in the film with rather small energy barriers. The water dissociates on the surface and induces the continuous presence of hydrogen atoms in the surface region during the growth process, which dynamically stabilizes the polar CaO(111) surface and facilitates the growth of CaO films along the polar [111] direction with arbitrary thicknesses. The controlled growth of polar CaO(111) provides opportunities to create new types of artificial heterostructures that lead to new interface science and new technology concepts. Finally, the surfactant-assisted growth method applied currently to polar CaO(111) film can be extended to more complicated systems, such as $BaTiO_3$ on $Al_{1-x}Ga_xN$, to create new integration possibilities and thus a new ability to harness the associated functionality.

ACKNOWLEDGMENTS

This work was supported by the US Department of Energy, Office of Science, Office of Basic Energy Sciences, Materials Sciences and Engineering Division under Contract No. DE-AC02-06CH11357. We acknowledge grants of computer time from EMSL, a national scientific user facility located at Pacific Northwest National Laboratory, Center for Nanoscale Materials located at Argonne National Laboratory, and the ANL Laboratory Computing Resource Center (LCRC). We would like to thank D. D. Fong for useful comments.

*Corresponding author: zapol@anl.gov

[1] J. Goniakowski, F. Finochi, and C. Noguera, Rep. Prog. Phys. **71**, 016501 (2008).
[2] C. Noguera, J. Phys.: Condens. Matter **12**, R367 (2000).
[3] J. Ciston, A. Subramanian, and L. D. Marks, Phys. Rev. B **79**, 085421 (2009).
[4] M. Gajdardziska-Josifovska, R. Plass, M. A. Schofield, D. R. Giese, and R. Sharma, J. Electron Microsc. **51**, S13 (2002).
[5] F. Finocchi, A. Barbier, J. Jupille, and C. Noguera, Phys. Rev. Lett. **92**, 136101 (2004).
[6] D. Wolf, Phys. Rev. Lett. **68**, 3315 (1992).
[7] H. S. Craft, J. F. Ihlefeld, M. D. Losego, R. Collazo, Z. Sitar, and J. P. Maria, Appl. Phys. Lett. **88**, 212906 (2006).
[8] T. L. Goodrich, J. Parisi, Z. Cai, and K. S. Ziemer, Appl. Phys. Lett. **90**, 042910 (2007).
[9] B. P. Gila, A. H. Onstine, J. Kim, K. K. Allums, F. Ren, C. R. Abernathy, and S. J. Pearton, J. Vac. Sci. Technol. B **21**, 2368 (2003).
[10] V. K. Lazarov, Z. Cai, K. Yoshida, K. H. L. Zhang, M. Weinert, K. S. Ziemer, and P. J. Hasnip, Phys. Rev. Lett. **107**, 056101 (2011).
[11] E. A. Paisley, M. D. Losego, B. E. Gaddy, J. S. Tweedie, R. Collazo, Z. Sitar, D. L. Irving, and J. P. Maria, Nature Communications **2**, 461 (2011).
[12] M. C. Righi, C. A. Pignedoli, R. Di Felice, C. M. Bertoni, and A. Catellani, Phys. Rev. Lett. **91**, 136101 (2003).
[13] G. Kresse and J. Hafner, Phys. Rev. B **49**, 14251 (1994).
[14] G. Kresse and D. Joubert, Phys. Rev. B **59**, 1758 (1999).
[15] J. P. Perdew, K. Burke, and M. Ernzerhof, Phys. Rev. Lett. **77**, 3865 (1996).
[16] *Landolt–Börnstein Tables*, edited by K. H. Hellwege and A. M. Hellwege, Group III, Vol. 7b1 (Springer, Berlin, 1975).
[17] H. J. Monkhorst and J. D. Pack, Phys. Rev. B **13**, 5188 (1976).
[18] G. Henkelman, B. P. Uberuaga, and H. Jónsson, J. Chem. Phys. **113**, 9901 (2000).